



Study of solar and other unknown anti-neutrino fluxes with Borexino at LNGS

Borexino Collaboration

G. Bellini^{i,1}, J. Benzigerⁿ, S. Bonettiⁱ, M. Buizza Avanziniⁱ, B. Caccianigaⁱ, L. Cadonati^p, F. Calaprice^m, C. Carraro^c, A. Chavarria^m, A. Chepurinov^j, D. D'Angeloⁱ, S. Davini^c, A. Derbin^o, A. Etenko^g, K. Fomenko^{b,h}, D. Francoⁱ, C. Galbiati^{m,2}, S. Gazzana^h, C. Ghiano^h, M. Giammarchiⁱ, M. Goeger-Neff^k, A. Goretti^m, E. Guardincerri^c, S. Hardy^q, Aldo Ianni^h, Andrea Ianni^m, M. Joyce^q, V.V. Kobychhev^e, D. Korablev^b, Y. Koshio^h, G. Korga^h, D. Kryn^a, M. Laubenstein^h, T. Lewke^k, E. Litvinovich^g, B. Loer^m, P. Lombardiⁱ, L. Ludhovaⁱ, I. Machulin^g, S. Manecki^q, W. Maneschg^d, G. Manuzio^c, Q. Meindl^k, E. Meroniⁱ, L. Miramontiⁱ, M. Miasiazek^f, D. Montanari^{h,m}, V. Muratova^o, L. Oberauer^k, M. Obolensky^a, F. Ortica^l, M. Pallavicini^c, L. Papp^h, L. Perassoⁱ, S. Perasso^c, A. Pocar^p, R.S. Raghavan^q, G. Ranucciⁱ, A. Razeto^h, A. Reⁱ, P. Risso^c, A. Romani^l, D. Rountree^q, A. Sabelnikov^g, R. Saldanha^m, C. Salvo^c, S. Schönert^d, H. Simgen^d, M. Skorokhvatov^g, O. Smirnov^b, A. Sotnikov^b, S. Sukhotin^g, Y. Suvorov^h, R. Tartaglia^h, G. Testera^c, D. Vignaud^a, R.B. Vogelaar^q, F. von Feilitzsch^k, J. Winter^k, M. Wojcik^f, A. Wright^m, M. Wurm^k, J. Xu^m, O. Zaimidoroga^b, S. Zavatarelli^c, G. Zuzel^d

^a Laboratoire AstroParticule et Cosmologie, 75231 Paris cedex 13, France

^b Joint Institute for Nuclear Research, 141980 Dubna, Russia

^c Dipartimento di Fisica, Università e INFN, Genova 16146, Italy

^d Max-Planck-Institut für Kernphysik, 69029 Heidelberg, Germany

^e Institute for Nuclear Research, 03680 Kiev, Ukraine

^f M. Smoluchowski Institute of Physics, Jagiellonian University, 30059 Krakow, Poland

^g RRC Kurchatov Institute, 123182 Moscow, Russia

^h INFN Laboratori Nazionali del Gran Sasso, SS 17 bis Km 18+910, 67010 Assergi (AQ), Italy

ⁱ Dipartimento di Fisica, Università degli Studi e INFN, 20133 Milano, Italy

^j Institute of Nuclear Physics, Lomonosov Moscow State University, 119899 Moscow, Russia

^k Physik Department, Technische Universität Muenchen, 85747 Garching, Germany

^l Dipartimento di Chimica, Università e INFN, 06123 Perugia, Italy

^m Physics Department, Princeton University, Princeton, NJ 08544, USA

ⁿ Chemical Engineering Department, Princeton University, Princeton, NJ 08544, USA

^o St. Petersburg Nuclear Physics Institute, 188350 Gatchina, Russia

^p Physics Department, University of Massachusetts, Amherst, MA 01003, USA

^q Physics Department, Virginia Polytechnic Institute and State University, Blacksburg, VA 24061, USA

ARTICLE INFO

Article history:

Received 4 October 2010

Received in revised form 6 December 2010

Accepted 20 December 2010

Available online 23 December 2010

Editor: L. Rolandi

Keywords:

Anti-neutrinos

Solar neutrinos

Neutrino detector

Liquid scintillator

ABSTRACT

We report on the search for anti-neutrinos of yet unknown origin with the Borexino detector at the Laboratori Nazionali del Gran Sasso. In particular, a hypothetical anti-neutrino flux from the Sun is investigated. Anti-neutrinos are detected through the neutron inverse β decay reaction in a large liquid organic scintillator target. We set a new upper limit for a hypothetical solar $\bar{\nu}_e$ flux of $760 \text{ cm}^{-2} \text{ s}^{-1}$, obtained assuming an undistorted solar ${}^8\text{B}$ energy spectrum. This corresponds to a limit on the transition probability of solar neutrinos to anti-neutrinos of 1.3×10^{-4} (90% C.L.) for $E_{\bar{\nu}} > 1.8 \text{ MeV}$, covering the entire ${}^8\text{B}$ spectrum. Best differential limits on anti-neutrino fluxes from unknown sources are also obtained between the detection energy threshold of 1.8 MeV and 17.8 MeV with more than 2 years of data.

© 2010 Elsevier B.V. All rights reserved.

The Borexino Collaboration has recently published a measurement of electron anti-neutrino fluxes at the Laboratori Nazionali del Gran Sasso (LNGS) [1]. Contributions from two known sources were observed: 1) $\bar{\nu}_e$'s produced in nuclear reactors and 2) geo-neutrinos, produced in β decays of isotopes along the decay chains of long-lived ^{238}U and ^{232}Th distributed within the Earth's interior. An $\bar{\nu}_e$ rate of $4.3^{+1.7}_{-1.4}$ events/(100 ton yr) was measured from nuclear reactors, consistent with an expected rate of 5.7 ± 0.3 events/(100 ton yr). Geo-neutrinos were identified at a rate of $3.9^{+1.6}_{-1.3}$ events/(100 ton yr).

In this Letter we present a study of other possible anti-neutrino sources. These include the search for hypothetical solar anti-neutrinos and the investigation of other, unspecified and model-independent $\bar{\nu}_e$ fluxes. A weak anti-neutrino flux from the Sun arising from $\bar{\nu}_e \rightarrow \nu_e$ conversion cannot be completely excluded with current experimental data. In particular, the interplay of flavor oscillations and spin flavor precession (SFP) induced by solar magnetic fields on Majorana neutrinos with sizable electric or magnetic transition moments [2–14] could lead to the appearance of an $\bar{\nu}_e$ admixture in the solar neutrino flux.

The current best limit on the solar anti-neutrino flux is $\phi_{\bar{\nu}_e} < 370 \text{ cm}^{-2} \text{ s}^{-1}$ (90% C.L.), reported by KamLAND [15]. The analysis was performed in the $8.3 < E_{\bar{\nu}_e} < 14.8$ MeV energy range. Assuming the undistorted solar ^8B spectrum, the limit on the anti-neutrino flux scaled to the entire energy range is $\phi_{\bar{\nu}_e} < 1250 \text{ cm}^{-2} \text{ s}^{-1}$ (90% C.L.), and a limit on the conversion probability $p_{\nu \rightarrow \bar{\nu}} < 2.8 \times 10^{-4}$ (90% C.L.) was set using the ^8B theoretical solar neutrino flux of $5.05^{+0.20}_{-0.16} \times 10^6 \text{ cm}^{-2} \text{ s}^{-1}$ [16].³ The expected background from known sources for this search in the energy range of interest was 1.1 ± 0.4 events/(0.28 ktyr) and no candidate events were observed in 185 days of data taking.

Although a smaller detector than KamLAND, Borexino has a competitive sensitivity in the high energy portion of the anti-neutrino energy spectrum, above reactor anti-neutrinos. At lower energies, Borexino compensates its size disadvantage with a significantly lower anti-neutrino background, due to its large distance from nuclear power plants (the average baseline is ~ 1000 km) and with lower intrinsic radioactive background.

Borexino [18–20] is a large volume, unsegmented organic liquid scintillator detector located underground at the Laboratori Nazionali del Gran Sasso, Italy. Primarily designed for a real-time, high precision measurement of the mono-energetic (862 keV) ^7Be solar neutrino flux via $\nu - e$ elastic scattering interactions in the scintillator, Borexino is also an extremely sensitive anti-neutrino detector. It began data taking in May 2007 and has already presented a measurement of the ^7Be solar neutrino flux with 10% precision [21]. Because both β and γ interactions are essentially indistinguishable from the sought-after neutrino induced events, the measurement was possible thanks to the high purity from radioactive contaminants achieved in the scintillator and surrounding detector components, $(1.6 \pm 0.1) \times 10^{-17} \text{ g/g}$ for ^{238}U and $(6.8 \pm 1.3) \times 10^{-18} \text{ g/g}$ for ^{232}Th [21].

A central spherical core of 278 tons (design value) of organic liquid scintillator (LS) solution, constituted of pseudocumene solvent (1,2,4-trimethylbenzene $\text{C}_6\text{H}_3(\text{CH}_3)_3$) doped with PPO fluor (2,5-diphenyloxazole, $\text{C}_{15}\text{H}_{11}\text{NO}$) with a concentration of 1.5 g/l, is contained within a 8.5 m-diameter thin transparent nylon ves-

sel (Inner Vessel, IV) and viewed by 2212 large area 8" photomultiplier tubes (PMTs) defining the inner detector (ID) and providing 34% geometric coverage. The scintillator is immersed in ~ 1000 tons of pseudocumene buffer fluid, divided into two regions by a second transparent nylon vessel 11.5 m in diameter, which prevents radon gas to permeate into the scintillator. Scintillator and buffer fluid are contained within a 13.7 m-diameter stainless steel sphere (SSS) on which the inward-looking PMTs are mounted. DMP (dimethylphthalate) dissolved in the buffer fluid quenches undesired scintillation from residual radioactivity contained in the SSS and PMTs. The SSS is immersed in a large water tank (WT) for further shielding from high energy γ rays and neutrons emerging from the surrounding rock. The WT is instrumented as a Čerenkov muon detector (outer detector, OD) with additional 208 PMTs, particularly important for detecting muons skimming the central detector inducing signals in the energy region of interest for neutrino physics. A detailed description of the Borexino detector can be found in Refs. [19,20].

A high light yield of $\simeq 500$ photoelectrons (p.e.) detected for every 1 MeV of electron energy deposited gives an energy resolution of $\sim 5\%$ at 1 MeV. The position of each scintillation event in Borexino is determined from the timing pattern of hit PMTs with a spatial reconstruction algorithm. The code has been tuned using data from several calibration campaigns with radioactive sources inserted at different positions inside the detector. A maximum deviation of 5 cm between the reference and reconstructed source positions is observed at a radius of ~ 4 m, close to the bottom of the IV.

In Borexino, anti-neutrinos are detected via the neutron inverse β decay reaction, $\bar{\nu}_e + p \rightarrow n + e^+$, with a kinematic threshold $E_{\bar{\nu}} > 1.8$ MeV. The cross section for this process is much higher than for $\bar{\nu} - e$ elastic scattering, making it the dominant anti-neutrino interaction in proton-rich water-Čerenkov and liquid scintillator detectors. This process also offers an experimentally unique signature given by the close time sequence of correlated events. The positron promptly annihilates emitting two 511 keV γ -rays, providing the prompt event, with a visible energy of $E_{\text{prompt}} = E_{\bar{\nu}} - 0.782$ MeV (the scintillation light related to the proton recoil is highly quenched and negligible). The neutron quickly thermalizes and is then captured by a proton after a time characteristic of the medium, via the reaction $n + p \rightarrow d + \gamma$. For protons, the de-excitation γ ray is 2.2 MeV and constitutes the delayed event. For the Borexino scintillator the mean capture time was measured to be $\sim 256 \mu\text{s}$. The coincident nature of anti-neutrino events allows for the detection of relatively few events with high significance. Incidentally, the 2.2 MeV photon is detected with low efficiency in water-Čerenkov detectors.

For the present analysis we used two anti-neutrino candidates selection criteria. With data set A, we selected anti-neutrinos candidates in the entire scintillator volume from the data collected between May 2007 and June 2010. The live time for set A after all analysis cuts is 736 days. Data set B coincides with the one used for the geo-neutrino analysis [1] and includes data taken between December 2007 and December 2009, for a total 482 days of live time. Analogously to what was done for the geo-neutrino analysis, a fiducial volume cut, detailed below, was introduced for data set B in order to suppress neutron background from $^{13}\text{C}(\alpha, n)^{16}\text{O}$ reactions initiated by ^{210}Po α decays in the non-scintillating buffer fluid surrounding the scintillator.

The following anti-neutrino candidates selection criteria have been defined based on calibration data and Monte Carlo (MC) simulations and applied to the data. All cuts apply to both data sets unless otherwise noted.

E-mail address: Gianpaolo.Bellini@mi.infn.it (G. Bellini).

¹ Spokesperson.

² Also at Fermi National Accelerator Laboratory, Batavia, IL 60510, USA.

³ In order to make the comparison of results clearer, we underline that the value for the ^8B flux used in current work is $5.88 \times 10^6 \text{ cm}^{-2} \text{ s}^{-1}$ [17].

1. $Q_{\text{prompt}} > 410$ p.e.; for reference, $Q = 438 \pm 2$ p.e. corresponds to the positron annihilation at rest with $E = 1.022$ MeV released at the center of the detector.
2. $700 < Q_{\text{delayed}} < 1250$ p.e.; 2.2 MeV γ 's deposit 1060 ± 5 p.e. at the detector's center; the lower limit is justified because photons at the edge of the scintillator can escape depositing none or only a fraction of their total energy).
3. $20 < \Delta T < 1280$ μs , where ΔT is the time between prompt and delayed event. The upper limit is 5 times the mean neutron capture time and guarantees good acceptance. The lower limit excludes double cluster events, i.e. events that fall within the same data acquisition gate, which present higher background contamination.
4. Reconstructed distance between prompt and delayed events: $\Delta R < 1$ m for data set B, $\Delta R < 1.5$ m for data set A to increase the acceptance.
5. $R_{\text{prompt}} < R_{\text{IV}}(\theta, \phi) - 0.25$ m for data set B, where R_{prompt} is the reconstructed radius for the prompt event and $R_{\text{IV}}(\theta, \phi)$ is the inner vessel radial size in the direction (θ, ϕ) of the event (the IV is not exactly spherical; its true shape is reconstructed using seven CCD cameras mounted on the SSS). No volume cut is applied for data set A.
6. All tagged muon events are dropped. Muons can cause events which mimic $\bar{\nu}_e$ events as illustrated in [1]. Cosmic muons are typically identified by the OD, but can also be distinguished from point-like scintillation events by the pulse shape analysis of the ID signal. The probability to miss a muon after identification by the OD and pulse shape analysis is 3×10^{-5} [1].
7. A 2 ms veto is applied after each muon which crosses the outer but not the inner detector in order to suppress background from fast neutrons produced along their tracks in water.
8. A 2 second veto is applied after each muon crossing the inner detector to suppress the $\beta - n$ decaying cosmogenic isotopes ${}^9\text{Li}$ ($\tau = 260$ ms) and ${}^8\text{He}$ ($\tau = 173$ ms).

Approximately 4300 muons traverse the ID every day, and an equivalent amount cross the OD alone. Cuts 6 and 7 thus introduce a modest dead time. Cut 8 corresponds to ~ 8600 seconds of dead time per day, or about 10%. A careful study of cuts 6–8 yielded a total dead time of 10.5%. The combined acceptance ϵ of all other cuts (1–4) is estimated by MC means at $(85 \pm 1)\%$ for data set B and $(83 \pm 1)\%$ for data set A, mostly attributable to the ΔT ($\epsilon = 91.8\%$) and ΔR ($\epsilon \sim 95\%$) cuts, and partially due to the loss of γ rays close to the IV surface.

The energy of each event is reconstructed using the total amount of light registered by all PMTs of the detector (measured in photoelectrons, p.e.) and corrected with a position-dependent light collection function $f(x, y, z)$, which relates the light yield at point (x, y, z) to that of the same event at the center of the detector, $Q(x, y, z) = f(x, y, z)Q_0$. An extensive calibration campaign with a set of gamma sources has been performed (the energy of the gamma rays ranged between a few hundred keV to 9 MeV). For events at the center of the detector, the total amount of light collected is linear with energy above 1 MeV [22]. The $f(x, y, z)$ function was constructed using calibration data from sources deployed at different positions inside the detector and checked against MC simulations. The correction is up to 15% at the poles of the detector, where scintillation light is shadowed the most by the conduits used to fill the detector. The estimated (systematic) uncertainty of the energy reconstruction procedure is about 2%. It is mainly due to the uncertainty in the $f(x, y, z)$ function, with a small contribution from the stability of the energy scale of the detector. The most energetic anti-neutrino candidate event in the entire data set has a total light yield $Q_{\text{prompt}} = 2996$ p.e. and is located within

the fiducial volume defined for data set B. $Q_{\text{prompt}} = 2996$ p.e. corresponds to $Q_0 = 2991$ p.e. at the center of the detector, or $E = 6.22 \pm 0.12$ (syst) MeV.

We looked for an admixture of anti-neutrinos within the solar neutrino flux, considering the case of energy independent conversion. Data set A was used for this analysis, with a threshold of 6.5 MeV for the visible energy (corresponding to an anti-neutrino energy of 7.3 MeV). With this threshold, the expected background in data set A is mainly due to the high energy tail of reactor anti-neutrinos, is estimated at $N_R = 0.31 \pm 0.02$ events. Additional backgrounds are hard to define and quantify, but in a conservative approach we can simply use the lowest possible value, i.e. zero background. The absence of anti-neutrino candidates in the entire 270 ± 3 tons of scintillator (as calculated by reconstructing the exact shape of the IV by means of images taken with seven inward-looking CCD cameras mounted on the SSS) during an observation time of $T = 736$ days is then used to set the following limit on a hypothetical solar anti-neutrino flux:

$$\phi_{\text{lim}} = \frac{S_{\text{lim}}}{\bar{\sigma} \cdot T \cdot N_p \cdot \epsilon} \text{ cm}^{-2} \text{ s}^{-1}, \quad (1)$$

where $N_p = (1.62 \pm 0.02) \times 10^{31}$ is the number of target protons, $\bar{\sigma}$ is the average cross section for neutron inverse beta decay [23] weighted over the ${}^8\text{B}$ solar neutrino spectrum [24] in the energy range of interest, S_{lim} is the maximum allowed signal at 90% C.L. and $\epsilon = 0.83 \pm 0.01$ is the efficiency (constant within the chosen interval) of inverse beta-decay detection for the chosen set of selected cuts, defined with MC simulation.

Assuming an undistorted solar ${}^8\text{B}$ neutrino energy spectrum $\bar{\sigma}(E_{\bar{\nu}} > 7.3) = 6.0 \times 10^{-42} \text{ cm}^2$ and with $S_{\text{lim}} = 2.13$, obtained applying the Feldman-Cousins procedure [25] for the case of no observed events with 0.31 expected background events we obtain:

$$\phi_{\bar{\nu}}({}^8\text{B}, E > 7.3 \text{ MeV}) < 415 \text{ cm}^{-2} \text{ s}^{-1} \text{ (90\% C.L.)}$$

Part of the spectrum above 7.3 MeV corresponds to 42% of the total ${}^8\text{B}$ neutrino spectrum [24], equivalently $\phi_{\bar{\nu}}({}^8\text{B}) < 990 \text{ cm}^{-2} \text{ s}^{-1}$ at 90% C.L. over the entire ${}^8\text{B}$ neutrino spectrum. This corresponds to an average transition probability in this energy range of $p_{\nu \rightarrow \bar{\nu}} < 1.7 \times 10^{-4}$ obtained assuming $\phi_{\text{SSM}}({}^8\text{B}) = 5.88 \times 10^6 \text{ cm}^{-2} \text{ s}^{-1}$ [17] (we do not take into account the errors on the theoretical predictions of the ${}^8\text{B}$ neutrino flux).

A limit was alternatively obtained using data set B over the entire ${}^8\text{B}$ spectrum. The reduced statistics due to the lower target fiducial volume ($N_p = 1.34 \times 10^{31}$), shorter data taking period ($T = 482$ days) and lower acceptance on ΔR with respect to data set A is partially compensated by the larger energy range and a higher detection efficiency, $\epsilon = 0.85 \pm 0.01$. Applying the fit procedure developed for the geo-neutrino studies [1] and following the χ^2 profile as a function of the amount of additional, hypothetical, anti-neutrinos under the assumption of an energy-independent ${}^8\text{B}$ solar neutrino conversion to anti-neutrino, we obtain $S_{\text{lim}} = 2.90$ at 90% C.L. From (1) and with $\bar{\sigma}(E_{\bar{\nu}} > 1.8) = 3.4 \times 10^{-42} \text{ cm}^2$:

$$\phi_{\bar{\nu}}({}^8\text{B}) < 1820 \text{ cm}^{-2} \text{ s}^{-1} \text{ (90\% C.L.)}$$

or $p_{\nu \rightarrow \bar{\nu}} < 3.1 \times 10^{-4}$ in the energy range above 1.8 MeV. This limit is weaker than that obtained by simple scaling of the result from the study above 7.3 MeV.

The strongest limit was obtained combining both data sets (below/above 7.3 MeV we used the data sets B/A, respectively). We applied the fit procedure developed for the geo-neutrino studies [1] with the ${}^8\text{B}$ neutrino spectrum correctly weighted for effective exposures below and above 7.3 MeV. Following the χ^2 profile with respect to the amount of additional hypothetical anti-neutrinos

Table 1

Limits on the $\bar{\nu}$ flux with undistorted ^8B spectrum for the Borexino, its prototype CTF, KamLAND, SNO and SuperKamiokaNDE experiments. Upper limits are given at 90% C.L. (see text for details).

Experiment	Measurement threshold [MeV]	Total $\phi_{\bar{\nu}_e} (^8\text{B})$ 90% C.L. [$\text{cm}^{-2} \text{s}^{-1}$]
CTF [39]	> 1.8	< 1.1×10^5
SNO [27]	> 4	< 4.09×10^4
SuperK [26]	> 8	< 4.04×10^4
KamLAND [15]	> 8.3	< 1250
Borexino (this work)	> 7.3	< 990
Borexino (this work)	> 1.8	< 760

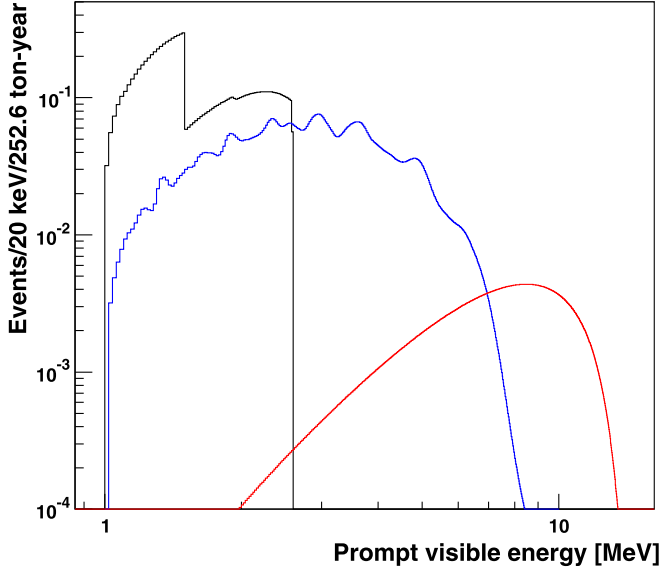


Fig. 1. Energy spectra for electron anti-neutrinos in Borexino. The horizontal axis shows the kinetic plus the annihilation 1.022 MeV energy of the prompt positron event. Shown are expected shapes for geo- (black line) and reactor (blue line) anti-neutrinos normalized to the Borexino measured values [1] for a 252.6 ton year exposure. Effects of neutrino oscillations are included. The spectral shape for hypothetical ^8B solar anti-neutrinos is shown in red and normalized to our upper limit of $1.3 \times 10^{-4} \phi_{SSM} (^8\text{B})$ (see text for details).

assuming an energy-independent ^8B neutrino conversion to anti-neutrino, we obtain $S_{\text{lim}} = 2.07$ at 90% C.L. (the corresponding fraction above 7.3 MeV is 1.64). Using (1) with $\bar{\sigma} = 6.0 \times 10^{-42} \text{ cm}^2$

$$\phi_{\bar{\nu}} (^8\text{B}, E > 7.3 \text{ MeV}) < 320 \text{ cm}^{-2} \text{Ps}^{-1} \text{ (90\% C.L.)},$$

which in the total energy range corresponds to:

$$\phi_{\bar{\nu}} (^8\text{B}) < 760 \text{ cm}^{-2} \text{s}^{-1} \text{90\% C.L.},$$

or $p_{\nu \rightarrow \bar{\nu}} < 1.3 \times 10^{-4}$ for the total ^8B flux. This limit is stronger than that obtained by simple scaling of the result from the study above 7.3 MeV energy range. Our limits for $\bar{\nu}$ flux with undistorted solar ^8B neutrino spectrum are summarized in Table 1, where they are compared with those reported by SuperKamiokaNDE [26], KamLAND [15] and SNO [27]. The upper limit on a hypothetical solar anti-neutrino rate is illustrated against the Borexino measured reactor and geo-neutrino rates [1] in Fig. 1.

The limit on solar anti-neutrinos allows us to set limits on the neutrino magnetic moment μ_ν and on the strength and shape of the solar magnetic field. Assuming the SFP mechanism coupled with the MSW-LMA solar neutrino solution, limits on the neutrino magnetic moment μ_ν can be obtained using the limits on the conversion probability $p_{\nu \rightarrow \bar{\nu}}$, as shown in [8–10]. In general,

the limit on μ_ν depends on the unknown strength of the solar magnetic field B in the neutrino production region, and can be written as [8]:

$$\mu_{\bar{\nu}} \leq 7.4 \times 10^{-7} \left(\frac{p_{\nu \rightarrow \bar{\nu}}}{\sin^2 2\theta_{12}} \right)^{1/2} \frac{\mu_B}{B_\perp [\text{kG}]}$$

where μ_B is Bohr's magneton and B_\perp is the transverse component of the solar magnetic field at a radius $0.05R_\odot$ corresponding to the maximum of ^8B -neutrino production. Using our experimental limit $p_{\nu \rightarrow \bar{\nu}} = 1.3 \times 10^{-4}$ and $\sin^2 2\theta_{12} = 0.86$ [28,29] one obtains $\mu_{\bar{\nu}} \leq 9 \times 10^{-9} B_\perp \mu_B$ (90% C.L.). Solar physics provides very limited knowledge on magnitude and shape of solar magnetic fields. In accordance with [30–32] the magnetic field in the core can vary between 600 G and 7 MG. The higher value limits the magnetic moment to $\mu_{\bar{\nu}} \leq 1.4 \times 10^{-12} \mu_B$.

The spin flip could also occur in the convective zone of the Sun in which neutrinos traverse a region of random turbulent magnetic fields [11–13]. Using the expression for the conversion probability given in [13,33] and the solar neutrino mixing parameters $\cos^2 \theta_{12} = 0.688$ and $\Delta m^2 = 7.64 \times 10^{-5} \text{ eV}^2$ [28,29], the limit on the magnetic moment can be written as:

$$\mu_{\bar{\nu}} \leq 8.2 \times 10^{-8} p_{\nu \rightarrow \bar{\nu}}^{1/2} B^{-1} [\text{kG}] \mu_B$$

where B is the average strength of the turbulent magnetic field. Using conservative values for B of 10–20 kG [12,13,33,34], we obtain less stringent limits on the magnetic moment than current laboratory bounds.

Currently, the best limit on the neutrino magnetic moment, $\mu_\nu < 3 \times 10^{-12} \mu_B$, is obtained by imposing astrophysical constraints that avoid excessive energy losses by globular-cluster stars [35]. The best direct limit is obtained with reactor neutrinos, $\mu_{\bar{\nu}_e} < 3.2 \times 10^{-11} \mu_B$ [36]. It has been claimed recently [37] that taking into account the effect of atomic ionization leads to significantly stronger constraints on magnetic moment ($\mu_{\bar{\nu}_e} < 5 \times 10^{-12} \mu_B$ [36, 37]), but according to [38] the neutrino–electron scattering cross section is not affected essentially by the atomic effects down to the energies transfer within the range of interest for the present experiments and the contribution of atomic ionization effect may be negligible.

The best limit on the effective magnetic moment of solar neutrinos is close, $\mu_\nu < 5.4 \times 10^{-11}$ (90% C.L.) [21]. It was obtained by the Borexino Collaboration by studying the shape of the electron recoil energy spectrum following elastic scattering from mono-energetic ^7Be solar neutrinos. These experimental limits on the neutrino magnetic moments, together with reasonable assumptions on the distribution of turbulent magnetic fields in the Sun, corresponds to a conversion probability $p_{\nu \rightarrow \bar{\nu}} \sim 10^{-6}$, about two orders of magnitude lower than the sensitivity of present experiments.

The case of an undistorted ^8B anti-neutrino spectrum is a special case of $\nu \rightarrow \bar{\nu}$ conversion. For the more general case, a model-independent search for unknown anti-neutrino fluxes was performed in 1 MeV energy bins for $1.8 \text{ MeV} < E_{\bar{\nu}} < 17.8 \text{ MeV}$. This study was made possible by the extremely low background achieved by Borexino. The analysis consisted in setting the limits on any contribution of unknown origin in the anti-neutrino spectrum registered by Borexino. Data set B was used below 7.8 MeV (same region used in our recent study of geo-neutrinos), where reactor and geo-neutrinos positively contribute to the signal, with 21 detected candidate events [1]. Data set A was used above 7.8 MeV where, as mentioned earlier, no events were recorded allowing us to use the full scintillator volume and a more inclusive ΔR value between the prompt and delayed events. Decrease in the

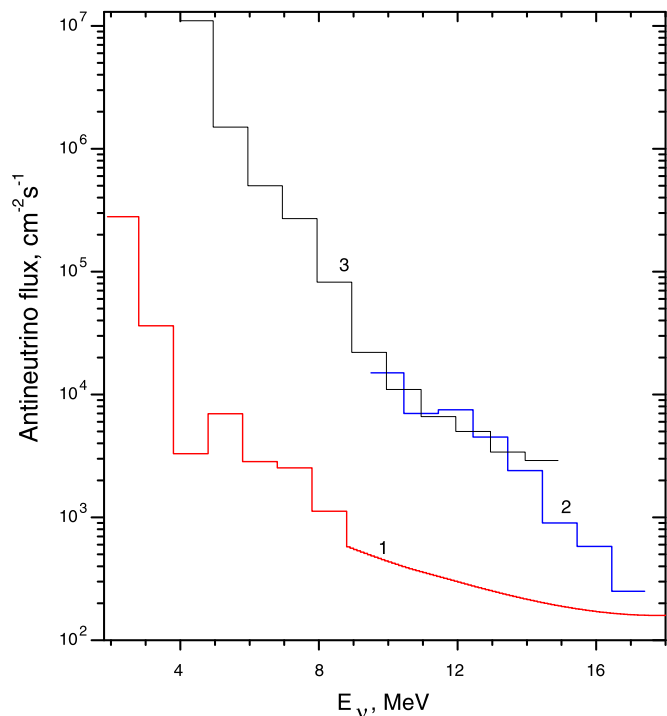


Fig. 2. Upper limits on the monochromatic $\bar{\nu}_e$ fluxes for: 1 – the present Borexino data (red line); 2 – SuperKamiokaNDE (blue line) [26] and 3 – SNO (black line) [27]. The regions above the lines are excluded. The x-axis is anti-neutrino energy.

detection efficiency at high energies due to muon software tagging over-efficiency via ID pulse shape analysis was considered and evaluated by MC simulations. The robustness of the event binning was tested against the precision of the light yield-to-energy conversion, which carries a 2% systematic uncertainty as mentioned earlier. The number of events assigned to each bin is not sensitive to the variation of parameters (within 90% C.L.) with the exception of bins 2 and 3. One event happens to be on the boundary of these two bins (within $\approx 0.5\%$ energy interval) and we conservatively assigned it to both in setting our limits.

In order to have conservative limits, the minimal expected number of events in every bin has been calculated separately for reactor and geo-neutrinos. For geo-neutrinos we considered the Minimal Radiogenic Earth model [40], which only includes the radioactivity from U and Th in the Earth crust which can be directly measured in rock-samples. More details on the calculation can be found in Ref. [1].

The 90% C.L. upper limits S_{lim} in the Feldman–Cousins approach for the first eight bins are {11.5, 6.48, 1.32, 4.93, 3.12, 3.96, 2.38, 2.43}, respectively. Above bin number 7 ($E > 7.8$ MeV) $S_{\text{lim}} = 2.44$, obtained with the Feldman–Cousins recipe for no observed events with zero background. Model independent limits on anti-neutrino fluxes are illustrated in Fig. 2 and compared with SuperKamiokaNDE [26] and SNO [27] data.

As far as concerned the possible conversion of the low energy neutrino below the 1.8 MeV inverse beta decay reaction threshold, including those that could originate by SFP conversion of the abundant ^7Be monoenergetic solar neutrinos, the only available detection channel is the elastic scattering on electrons. The recoil spectra for electrons elastically scattering off neutrino and anti-neutrinos are distinct, and we exploited such difference to search for an anti-neutrino admixture in the ^7Be solar neutrino flux. Possible deviations from the pure $\nu - e$ electron recoil shape due to electromagnetic interactions were studied in Borexino previ-

ously published data [21]. Following the changes in the χ^2 profile with respect to the addition of an anti-neutrino component we set a limit on the conversion probability for ^7Be solar neutrinos of $p_{\nu_e \rightarrow \bar{\nu}_e} < 0.35$ at 90% C.L. The relatively low sensitivity is in large part due to the strong anti-correlation between the $\bar{\nu} - e$ elastic scattering spectrum and that of ^{85}Kr (a β emitter which represents a significant residual background in Borexino) both left free in the analysis. It is likely that this limit could be improved following a purification campaign of the scintillator.

In conclusion, Borexino has shown excellent sensitivity to naturally-produced anti-neutrinos over a broad range of energies, thanks to its unprecedented radiological purity and its location far away from nuclear reactors. New limits have been set on the possible $\bar{\nu}$ admixture in the solar neutrino flux. In particular, $p_{\nu \rightarrow \bar{\nu}} < 1.7 \times 10^{-4}$ (90% C.L.) for $E_{\bar{\nu}} > 7.3$ MeV, $p_{\nu \rightarrow \bar{\nu}} < 1.3 \times 10^{-4}$ (90% C.L.) for the whole ^8B energy region, and $p_{\nu_e \rightarrow \bar{\nu}_e} < 0.35$ (90% C.L.) for 862 keV ^7Be neutrinos. The best differential limits on anti-neutrino fluxes of unknown origin between 1.8 and 17.8 MeV have also been set.

Acknowledgements

This work was funded by INFN (Italy), NSF (US Grant NSFPHY-0802646), BMBF (Germany), DFG (Germany, Grant OB160/1-1 and Cluster of Excellence “Origin and Structure of the Universe”), MPG (Germany), Rosnauka (Russia, RFBR Grant 09-02-92430), and MNiSW (Poland). This work was partially supported by PRIN 2007 protocol 2007 JR4STW from MIUR (Italy). O. Smirnov, L. Ludhova and A. Derbin acknowledge the support of Fondazione Cariplo.

References

- [1] G. Bellini, et al., Borexino Collaboration, Phys. Lett. B 687 (2010) 299.
- [2] J. Schechter, J.W.F. Valle, Phys. Rev. D 24 (1981) 1883; J. Schechter, J.W.F. Valle, Phys. Rev. D 25 (1982) 283, Erratum.
- [3] E.K. Akhmedov, Phys. Lett. B 213 (1988) 64.
- [4] C.S. Lim, W.J. Marciano, Phys. Rev. D 37 (1988) 1368.
- [5] R.S. Raghavan, et al., Phys. Rev. D 44 (1991) 3786.
- [6] E.K. Akhmedov, J. Pulido, Phys. Lett. B 529 (2002) 193.
- [7] J. Barranco, et al., Phys. Rev. D 66 (2002) 093009.
- [8] E.Kh. Akhmedov, J. Pulido, Phys. Lett. B 553 (2003) 7.
- [9] B.C. Chauhan, J. Pulido, E. Torrente-Lujan, Phys. Rev. D 68 (2003) 033015.
- [10] A.B. Balantekin, C. Volpe, Phys. Rev. D 72 (2005) 033008.
- [11] O.G. Miranda, T.I. Rashba, A.I. Rez, J.W.F. Valle, Phys. Rev. Lett. 93 (2004) 051304.
- [12] O.G. Miranda, T.I. Rashba, A.I. Rez, J.W.F. Valle, Phys. Rev. D 70 (2004) 113002.
- [13] A. Friedland, 2005, arXiv:hep-ph/0505165.
- [14] C. Giunti, A. Studenikin, Phys. Atom. Nucl. 72 (2009) 2089, arXiv:0812.3646v5 [hep-ph].
- [15] K. Eguchi, et al., KamLAND Collaboration, Phys. Rev. Lett. 92 (2004) 071301.
- [16] J.N. Bahcall, et al., Astrophys. J. 555 (2001) 990.
- [17] A.M. Serenelli, 2009, arXiv:0910.3690.
- [18] G. Alimonti, et al., Borexino Collaboration, Astropart. Phys. 16 (2002) 205.
- [19] G. Alimonti, et al., Borexino Collaboration, Nucl. Instr. and Methods A 600 (2009) 568.
- [20] G. Alimonti, et al., Borexino Collaboration, Nucl. Instr. and Methods A 609 (2009) 59.
- [21] C. Arpesella, et al., Borexino Collaboration, Phys. Rev. Lett. 101 (2008) 091302.
- [22] G. Bellini, et al., Borexino Collaboration, Phys. Rev. C 81 (2010) 034317.
- [23] A. Strumia, F. Vissani, Phys. Lett. B 564 (2003) 42.
- [24] J.N. Bahcall, et al., Phys. Rev. C. 54 (1996) 411.
- [25] G.J. Feldman, R.D. Cousins, Phys. Rev. D 57 (1998) 3873.
- [26] Y. Gando, et al., SuperKamiokaNDE Collaboration, Phys. Rev. Lett. 90 (2003) 171302.
- [27] B. Aharmim, et al., SNO Collaboration, Phys. Rev. D 70 (2004) 093014.
- [28] G.L. Fogli, et al., Phys. Rev. D 78 (2008) 033010.
- [29] M.C. Gonzalez-Garcia, M. Maltoni, J. Salvado, JHEP 1005 (2010) 072, arXiv:0910.4584v3.
- [30] L.L. Kitchatinov, Astron. Rep. 52 (2008) 247.
- [31] A. Friedland, A. Gruzinov, Astrophys. J. 601 (2004) 570.
- [32] H.M. Antia, J. Astrophys. Astr. 29 (2008) 85.

- [33] G. Raffelt, T. Rashba, *Phys. Atom. Nucl.* 73 (2010) 609, arXiv:0902.4832v1 [astro-ph.HE].
- [34] A. Friedland, A. Gruzinov, *Astropart. Phys.* 19 (2003) 575.
- [35] G. Raffelt, A. Weiss, *Astron. Astrophys.* 264 (1992) 536.
- [36] A.G. Beda, et al., arXiv:1005.2736v2, 2010.
- [37] H.T. Wong, H.-B. Li, S.-T. Lin, *Phys. Rev. Lett.* 105 (2010) 061801.
- [38] M.B. Voloshin, *Phys. Rev. Lett.* 105 (2010) 201801, arXiv:1008.2171v3.
- [39] M. Balata, et al., *Eur. Phys. J. C* 47 (2006) 21.
- [40] F. Mantovani, L. Carmignani, G. Fiorentini, M. Lissia, *Phys. Rev. D* 69 (2004) 013001.